Estimating heritability explained by local ancestry and evaluating stratification bias in admixture mapping from summary statistics

Tsz Fung Chan[1], Xinyue Rui[1], David V. Conti[1], Myriam Fornage[2], Mariaelisa Graff[3], Jeffrey Haessler[4], Christopher Haiman[1], Heather M. Highland[3], Su Yon Jung[5], Eimear Kenny[6], Charles Kooperberg[4], Loic Le Marchland[7], Kari E. North[3], Ran Tao[8,9], Genevieve Wojcik[10], Christopher R. Gignoux[11], PAGE Consortium, Charleston W. K. Chiang[1,12,*], Nicholas Mancuso[1,12,*]

1. Center for Genetic Epidemiology, Department of Population and Public Health Sciences, Keck School of Medicine, University of Southern California
2. Brown Foundation Institute for Molecular Medicine, The University of Texas Health Science Center, Houston, TX, USA
3. Department of Epidemiology, Gillings School of Global Public Health, University of North Carolina, Chapel Hill, North Carolina, United States of America
4. Division of Public Health Sciences, Fred Hutchinson Cancer Center, Seattle, WA, USA
5. Translational Sciences Section, School of Nursing, Jonsson Comprehensive Cancer Center, University of California, Los Angeles, Los Angeles, CA, United States
6. Institute for Genomic Health, Icahn School of Medicine at Mount Sinai, New York, NY, USA
7. Epidemiology Program, University of Hawaii Cancer Center, Honolulu, HI, USA
8. Department of Biostatistics, Vanderbilt University Medical Center, Nashville, TN, USA
9. Vanderbilt Genetics Institute, Vanderbilt University Medical Center, Nashville, TN, USA
10. Department of Epidemiology, Bloomberg School of Public Health, John Hopkins University, Baltimore, MD, USA
11. Colorado Center for Personalized Medicine, University of Colorado Anschutz Medical Campus, Aurora, CO, USA
12. Department of Quantitative and Computational Biology, University of Southern California

* co-supervised this work

Abstract

The heritability explained by local ancestry markers in an admixed population (h_γ^2) provides crucial insight into the genetic architecture of a complex disease or trait. Estimation of h_γ^2 can be susceptible to biases due to population structure in ancestral populations. Here, we present a novel approach, Heritability estimation from Admixture Mapping Summary STAtistics (HAMSTA), which uses summary statistics from admixture mapping to infer heritability explained by local ancestry while adjusting for biases due to ancestral stratification. Through extensive simulations, we demonstrate that HAMSTA h_γ^2 estimates are approximately unbiased and are robust to ancestral stratification compared to existing approaches. In the presence of ancestral stratification, we show a HAMSTA-derived sampling scheme provides a calibrated family-wise error rate (FWER) of ~5% for admixture mapping, unlike existing FWER estimation approaches. We apply HAMSTA to 20 quantitative phenotypes of up to 15,988 self-reported African American individuals in the Population Architecture using Genomics and Epidemiology (PAGE) study. We observe $\hat{h}_\gamma^2$ in the 20 phenotypes range from 0.0025 to 0.033 (mean $\hat{h}_\gamma^2$ = 0.012 +/- 9.2×10^{-4}), which translates to $\hat{h}^2$ ranging from 0.062 to 0.85 (mean $\hat{h}^2$ = 0.30 +/- 0.023). Across these phenotypes we find little evidence of inflation due to ancestral population stratification in current admixture mapping studies (mean inflation factor of 0.99 +/- 0.001). Overall, HAMSTA provides a fast and powerful approach to estimate genome-wide heritability and evaluate biases in test statistics of admixture mapping studies.

Introduction

Admixture mapping (AM) aims to identify genomic regions associated with a disease or quantitative trait in recently admixed populations[1–7] by leveraging the differences in allele frequencies between local ancestries[8]. AM provides a powerful approach to complement genome-wide association studies (GWAS) in admixed populations due to local ancestry information better tagging uncommon or poorly imputed causal variants[5] and spanning larger genomic regions, thus reducing the multiple testing burden[9], enabling discoveries with relatively smaller sample sizes [3,10]. Similarly, recent work[11] demonstrated that local ancestry information, which is summarized by heritability explained by local ancestry h_γ^2, can be leveraged to estimate narrow-sense heritability h^2 in admixed populations, unlike the genotype-based lower bounds (i.e. h_g^2). Multiple works have shown that population structure can bias association tests and estimates of h_g^2 [12,13]. However, it is less understood how similar demographic phenomena bias AM and h_γ^2 inference in admixed populations.

Admixed populations are typically modeled as a mixture of multiple continental ancestries (e.g., African, European, or Native American) with finer-scale structure within ancestral populations left unmodeled. Nevertheless, human populations are often structured across both space and time. For example, European ancestry individuals can be modeled as a mixture of at least three ancient populations[14], and Native American ancestry components found in Latinos can also be derived across multiple subpopulations spread across Latin America[15]. This unmodeled fine-scale structure could lead to potential biases in downstream association testing. Indeed, this phenomenon has been demonstrated in European populations [16,17], and could similarly impact inference in admixed populations when it is not fully accounted for [18]. When estimating ${h_g}^2$ using SNP data of large sample size, a robust approach to population stratification is to estimate h^2 and test statistic inflation simultaneously[19]. Examples of this approach include linkage disequilibrium score regression (LDSC)[13] and cov-LDSC[12]. While these methods are designed for SNP data, it remains unclear how applicable they are on estimating h_γ^2 using summary statistics from admixture mapping studies.

In this study we propose HAMSTA (Heritability estimation from Admixture Mapping Summary STAtistics), a novel likelihood-based approach to infer h_γ^2 from admixture mapping summary statistics. To achieve robust and efficient computation, HAMSTA transforms the correlated test statistics using a truncated singular value decomposition (tSVD) and performs maximum-likelihood inference while accounting for residual inflation due to stratification within ancestral populations. We perform extensive simulations and demonstrate that HAMSTA provides approximately unbiased estimates of h_γ^2 and outperforms existing approaches to detect evidence of stratification bias. We demonstrate estimates from HAMSTA can be leveraged to efficiently compute well-calibrated family-wise error rates for admixture mapping, particularly in presence of ancestral stratification which previous approaches do not consider [20]. Next, we apply HAMSTA to

admixture mapping summary statistics for 20 traits from 15,988 self-identified African American individuals in the Population Architecture using Genomics and Epidemiology (PAGE) study [21]. We find the h^2 estimates of 0.85 (0.085) and 0.42 (0.086) for height and BMI respectively. Compared with LDSC on admixture mapping summary statistics, HAMSTA offers more precise estimates for h_γ^2 and better quantifies the inflation in the test statistics due to unknown confounding biases. Overall, we demonstrate that HAMSTA provides a fast and powerful way to estimate genome-wide heritability that controls biases using summary statistics from admixture mapping studies.

Materials and Methods

Model for complex trait and ancestral stratification

We consider a two-way admixed population, with ancestral populations pop1 and pop2, which is recently structured into pop2a and pop2b (**Supplementary Figure 1**). This demographic model mimics the African and European admixture in African American and the finer-scale structure in their ancestral European population. We let γ, δ and $-\delta$ denote the population mean phenotype values of pop1, pop2a and pop2b. We denote $A_{i,k}$ as the centered and standardized local ancestry calls for individual *i* at marker *k*, such that $E[A_{i,k}] = 0$ and $Var[A_{i,k}] = 1$. We denote indexing over N individuals at the *k*th marker as A_k and index over M markers for the *i*th individual as A_i. We define the phenotype y_i of an admixed individual *i* as,

$$y_i = A_i\beta + \pi_i\gamma + d_i\delta + \epsilon_i ,$$

where β is the $M \times 1$ vector of local ancestry effects, π_i is defined as the global ancestry proportion due to pop1, $d_i = \pi_i^{(2a)} - \pi_i^{(2b)}$ is the difference between the global ancestry proportions of pop2a and pop2b, and $\epsilon_i \sim N(0, \sigma^2{}_\epsilon)$ is residual environmental noise. Furthermore, we assume that $\beta_k \sim N(0, \frac{h_\gamma^2}{M})$, where h_γ^2 is defined as the heritability explained by local ancestry [11]. Lastly, we define $\frac{\gamma^2}{n}\pi'\pi$ as the phenotypic variance explained (PVE) by global ancestry, and $\frac{\delta^2}{n}d'd$ as PVE by ancestral stratification.

Test statistics for admixture mapping

We model the marginal association statistics from an admixture mapping study where only global ancestry proportions π_i (and not d_i) are known beforehand. If the stratification term is not adjusted, the test statistics for marker *k* will be $Z_k = s_R{}^{-1}(A_k{}'PA_k)^{-1/2}(A_k{}'Py)$, where $s_R{}^2$is the residual variance after the global ancestry π is projected out by matrix $P = I - \pi(\pi'\pi)^{-1}\pi'$. Extending this to all *M* markers we have, $Z = s_R{}^{-1}D^{-1/2}(A'Py)$, where D is the diagonal elements of $A'PA$. Given this and distributional assumptions regarding y, we can derive the expectation and covariance of Z as,

$$E[Z] = s_R{}^{-1} D^{-1/2} A'Pd\delta$$

$$Cov[Z] = s_R{}^{-2} \left[\frac{h_\gamma^2}{M} D^{-1/2}(A'PA)^2 D^{-1/2} + (A'PA)\sigma_\epsilon^2\right].$$

The $D^{-1/2}(A'PA)D^{-1/2}$ is local ancestry disequilibrium (LAD) matrix analogous to the LD matrix and $D^{-1}(A'PA)^2D^{-1}$ is the LAD score matrix in which element (j,k) is approximately the dot product of correlation vectors of two markers j and k. When sample size N is large, the test statistics Z are well-approximated by a multivariate normal distribution. The mean reflects the bias due to correlation between local ancestry and ancestral stratification conditional on the global ancestry. In the covariance, the first term is related to the heritability explained by local ancestry and LAD score matrix. The second term in the covariance is related to LAD matrix and nongenetic effects. In the null scenario, where $h_\gamma^2 = 0$, $\delta = 0$, the distribution of Z has means of zeros and covariances simply equal to the LAD matrix.

We let the singular value decomposition (SVD) of $A'P = USV'$, $A'PA = US^2U'$ and $(A'PA)^2 = US^4U'$. We define rotation $Z^* = S^{-1}s_R U'D^{1/2}Z$, which follows $Z^* \sim N(V'd\delta, \frac{h_\gamma^2}{M} S^2 + \sigma_\epsilon^2)$, where the components are independent. We then assume $V'd\delta$ to be random and follow a normal distribution $N(0, C^*)$ such that $Z^* \sim N(0, \frac{h_\gamma^2}{M} S^2 + (\sigma_\epsilon^2 + C^*))$. The parameters h_γ^2 and "intercept" $C = (\sigma_\epsilon^2 + C^*)$ are the parameters to be inferred. To allow heterogeneous C across Z^*, we allow C to be different every 500 elements, i.e., $C = (c_1 \cdots_{\times 500}, c_2 \cdots_{\times 500}, \cdots)$. Test statistics from different chromosomes are rotated separately and do not share elements in C.

Inferring h_γ^2 and biases using HAMSTA

Parameters h_γ^2 and C were log-transformed to ensure positivity during optimization. First, we test for ancestral stratification using a likelihood ratio test between models with multiple intercepts and single intercepts in which C is a scalar shared by all elements in Z^*. If the test is significant with $p < 0.05$, we determine the maximum likelihood estimates $\hat{h}_\gamma^2$ and $\hat{C}$ under the multiple intercept model. Otherwise, we find $\hat{h}_\gamma^2$ and $\hat{C}$ under the single intercept model. To test for the significance of $\hat{h}_\gamma^2$, we use a likelihood ratio test that test the hypothesis $h_\gamma^2 = 0$. The standard errors of the estimates were determined using the jackknife method over 10 blocks.

Estimating h^2 from h_γ^2

Previous work[11] demonstrated a relationship between narrow-sense heritability h^2 and h_γ^2 as $h_\gamma^2 = 2F_{STC}\,\pi(1-\pi)\,h^2$. The F_{STC} is defined as the average genetic distance between the ancestral populations at causal loci. At each site, the genetic distance is computed as $\frac{(f_1-f_2)^2}{2f(1-f)}$,

where f_1, f_2 and f are the allele frequency in the ancestral populations and the admixed population. We provided h^2 estimates based on 1) F_{STC} = 0.1692 reported in the original study[11], which was estimated from HapMap 3 dataset and 2) F_{STC} = 0.1152 estimated in this study using a subset of African and European descent from the 1000 Genome and HGDP subset in gnomAD v3.1 [22], assuming common variants explain 90% of h^2 . The average admixture proportion π was observed to be 78% African ancestry.

Simulation design

To validate and assess performance of HAMSTA we performed simulations using realistic demographic scenarios. Specifically, we simulated ancestral populations *pop1* and *pop2* mirroring African and European populations in the Out-of-Africa demography model [23]. We additionally introduced structure into *pop2* by subdividing it into two subpopulations (denoted by *pop2a* and *pop2b* below, **Supplementary Figure 1**). We set *pop2a* and *pop2b* to have diverged 200 generations ago with a migration rate = 10^{-3}. These parameters were selected to result in a genetic differentiation similar to that within European populations ($F_{ST} \approx 0.003$) estimated from the HGDP and 1000 Genome subsets in gnomAD [22]. We simulated this demography for a 250Mb region with a uniform recombination rate of 10^{-8} per bp using msprime [24]. Using the true genealogies from simulations, we extracted the true local ancestry of each individual by tracing their lineage to each ancestral population (pop1, pop2a or pop2b). Global ancestries were computed from local ancestry information by computing the total proportion of the 250Mb region that is inherited from an ancestral population. We sampled 50,000 admixed individuals and 20,000 local ancestry markers according to the demography mode.

Next, we simulated phenotypes according to our phenotype model $y = A\beta + \pi\alpha + d\delta + \epsilon$. Given a sparsity α, we drew the effect of a local ancestry marker β_k from $N(0, \frac{h_\gamma^2}{\alpha M})$ with probability α and ϵ from $N(0, \sigma_\epsilon^2)$. Then we set the true h_γ^2 , PVE by global ancestry, PVE by ancestral stratification, and σ_ϵ^2 by varying the values of γ and δ. Finally, test statistics were computed using linear regression adjusting for π using PLINK 2.0 [25].

Estimate h_γ^2 with other approaches

To compare HAMSTA with existing methods in h_γ^2 estimation, we applied BOLT-REML[26], GCTA [27] and LD score regression (LDSC)[13] to the simulated and real-world data. In GCTA, the same set of covariates included in the admixture mapping were used in h_γ^2 estimation. Following previous studies, we compute the genetic relatedness matrix using local ancestry in place of genotypes [11]. In LDSC, we define the "local ancestry linkage disequilibrium" (LAD) score for marker i as $l_i = \sum_{j \in W} r_{i,j}^2$ with W being the set of markers in a given window size. Window sizes of 1-cM and 20-cM were used. The LAD scores were used as the regressors and weights in LDSC.

Significance threshold estimation

Specifically, to determine the significance threshold for a given admixture mapping study, we randomly generated test statistics $Z = s_R^{-1} D^{-1/2} USQ$, where Q is a vector of random variable sampled from $N(0, \sigma_q^2)$. We set σ_q^2 to be the maximum intercept if the test for multiple intercepts is significant, and σ_q^2 to be the inferred intercept if the test is not significant. We repeated the sampling procedure 2,000 times to determine the critical value as the 95% percentile of $max(Z^2)$. The significance threshold was determined as the tail probability of a chi-square distribution (degree of freedom = 1) at the critical value. To determine the threshold for multiple chromosomes, we estimate the threshold for each chromosome separately and then combine the thresholds by summing up the effective testing burden, i.e., $Combined\ thres = 0.05/\sum_{i=1}^{22}(0.05/thres_{chromosome\ i})$. For comparison, we also estimated the significance threshold using STEAM[20], which sampled from $Z = MVN(0, \Sigma)$, where Σ is a local ancestry correlation matrix based on genetic distance and admixture parameters. Family-wise error rates (FWER) were computed as the percentage of times at least one significant signal is identified out of 500 null simulations.

Local ancestry inference and genome-wide mapping for admixed individuals in PAGE cohort

We obtained phenotypes and genotyping data measured on Multi-Ethnic Genotyping Array (MEGA) from the PAGE study [21]. The complete dataset included 17,299 participants who self-identified as African American. Our analysis included 20 quantitative phenotypes: Body mass index (BMI), height, waist-to-hip ratio, diastolic blood pressure, systolic blood pressure, PR interval, QRS interval, QT interval, fasting glucose, fasting insulin, C-reactive protein, mean corpuscular hemoglobin concentration, platelet count, estimated glomerular filtration rate, cigarettes per day, coffee cups per day, high-density lipoprotein (HDL), low-density lipoprotein (LDL), triglycerides, and total cholesterol. Filters and transformations were applied, and covariates were selected according to the original PAGE analysis within the African American subset [21].

To infer the local ancestry, a subset of African and European genomes from the 1000 Genome and HGDP subset in gnomAD were used as reference individuals [22]. After filtering out SNPs with missingness > 10%, lifting over and merging, 516,731 SNPs were used in the local ancestry inference, resulting in 101,292 local ancestry markers. The genotypes of PAGE and reference individuals were re-phased together using EAGLE [28], and the ancestry probabilities were inferred as the local ancestry of the haplotype in a region using RFMIX2 [29]. The global ancestry of an individual was computed by taking the average of all predicted local ancestries. We analyzed up to 15,988 individuals who have >5% of one of the inferred ancestries and have no missing values in the covariates in the 20 quantitative phenotypes. Admixture mapping was performed using linear regression adjusting for the study center, inferred global ancestry, and phenotype-specific

covariates used in PAGE. The average estimate of h_γ^2 across phenotypes was calculated by weighting the estimate of each phenotype by the inverse of the squared standard error. The run time was measured on a machine with an Intel Xeon 4116 processor and 48GB memory.

Results

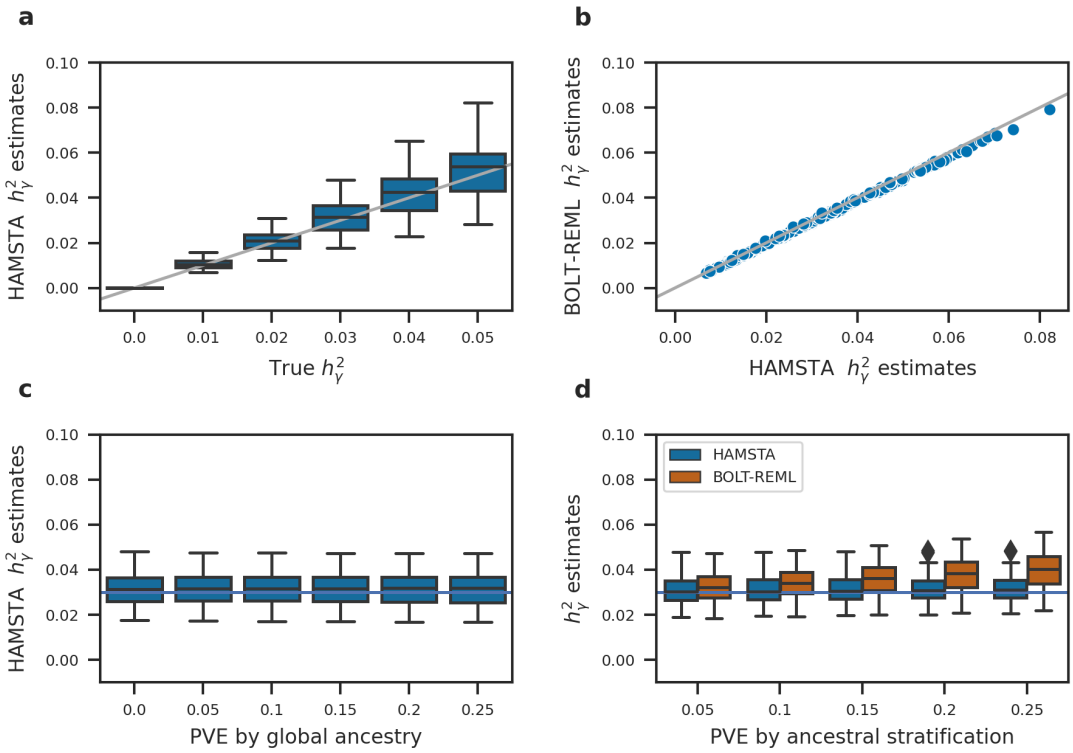

Figure 1

Simulation results from 50,000 admixed individuals and phenotypes under different levels of variance explained by local ancestry, global ancestry and ancestral stratification. The box plots show the range and quartiles of the estimates. a) Results of h_γ^2 estimation when varying true h_γ^2. Phenotypic variance explained (PVE) by global ancestry and ancestral stratification were set to 0. A gray identity line is plotted. b) Comparison of h_γ^2 estimates between HAMSTA and BOLT-REML applied to simulation data when true $h_\gamma^2 = \{0.01, 0.02, 0.03, 0.05\}$ in figure a. c) Results when varying the PVE by global ancestry, setting $h_\gamma^2 = 0.03$ (horizontal line) and PVE by ancestral stratification = 0. d) Comparison of h_γ^2 estimates between HAMSTA and BOLT-REML under various levels of ancestral stratification. True h_γ^2 were fixed at 0.03 (horizontal line).

HAMSTA provides unbiased estimates of h_γ^2 under ancestral stratification

To evaluate the accuracy of h_γ^2 estimates under various scenarios, we performed simulation studies using local ancestry data simulated under a population demographic model that mirrors African American admixture history with an addition of recent population structure in one of the ancestral populations (see **Methods**). Briefly, we simulated phenotypes absent stratification effects where we varied h_γ^2 from 0 to 0.05 (corresponding to h^2 from 0 to 1 according to ref [11]), which reflects h_γ^2 estimates reported in previous African American samples [30], and performed admixture mapping to compute summary statistics. Overall, we found HAMSTA produced approximately unbiased estimates of h_γ^2 (**Figure 1a**), irrespective of the sparsity of causal markers (**Supplementary Figure 2**). We observed that the summary statistics- based estimates from HAMSTA were highly correlated with those computed from individual-level data using BOLT-REML (**Figure 1b**), suggesting that when stratification bias is not present, there is no loss in accuracy across data settings. Next, to compare our method with existing summary statistics-based methods, we applied LD score regression (LDSC; see **Methods**) and observed LDSC produced biased estimates exhibited large standard errors (**Supplementary Figure 3**). Importantly, we found LDSC estimates remained biased after re-estimating "LAD scores" using a larger window size of 20-cM (**Supplementary Figure 3**). Next, we varied effect of global ancestry while fixing the h_γ^2 and PVE by ancestral stratification and found HASMTA h_γ^2 estimates remained unbiased (**Figure 1c**). Together, our results suggest that when stratification does not inflate summary statistics, HAMSTA provides unbiased estimates of h_γ^2 , unlike existing summary-based approaches.

Next, we sought to evaluate HAMSTA in presence of ancestral stratifications. We determined that the h_γ^2 estimates in our method were more robust to the presence of unadjusted ancestral stratification (**Figure 1d**). In contrast, BOLT-REML, where the inference model is not aware of ancestral stratification, produced biased results as the PVE by ancestral stratification increases.

Further, we demonstrate that our method is still robust to other scenarios of structures in the ancestral populations (**Supplementary Figure 4**). We explored the cases where i) both ancestral populations are structured, ii) the proportion of ancestries from the subpopulations are unequal in the admixed population, ii) the subpopulations are introduced to the admixture event at different times. In all the scenarios, the unbiasedness of our estimator is not affected by the ancestral stratification.

Overall, we demonstrated HAMSTA provides unbiased estimates of h_γ^2 under various levels of effects from local ancestry, global ancestry, and stratification in ancestral populations.

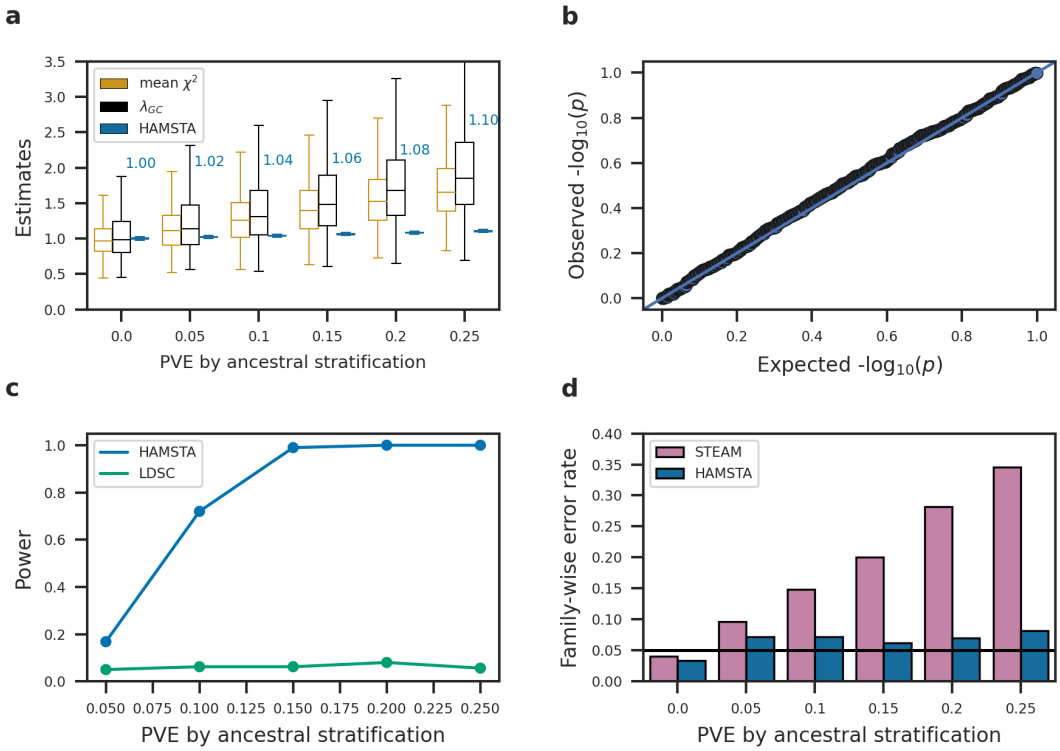

Figure 2

Evaluating ancestral stratification by HAMSTA in 500 simulation replicates. We simulated 50,000 admixed individuals and phenotypes under various levels of variance explained by local ancestral stratification. The true h_γ^2 is set to zero. a) Ancestral stratification is reflected by measures of test statistic inflation. The average estimates of HAMSTA's intercepts are labeled. b) Quantile-quantile plot of test statistics for the test for ancestral stratification. c) Power comparison between HAMSTA and LDSC in detecting ancestral stratification. The p value cutoff for each approach was determined such that the significance level = 0.05 in null simulation d) Family-wise error rate before and after correcting p-value cutoff in admixture mapping using the estimated intercepts.

HAMSTA estimates inflation in admixture mapping statistics due to stratification

Having established the unbiasedness in h_γ^2 estimates, we next sought to evaluate the ability of HAMSTA to identify inflation in admixture mapping statistics due to ancestral population stratification. Specifically, intercepts estimated by HAMSTA can be tested against the null (i.e., 1) to evaluate stratification bias. Overall, we observed HAMSTA produced estimates greater than 1 as the PVE by ancestral stratification increased (**Figure 2a**), demonstrating the ability of HAMSTA inferred intercepts to capture stratification-induced inflation. Although we noted similar trends in other measures of inflation, including mean χ^2, genomic inflation factor λ_{GC}, their inability to distinguish between polygenicity and confounding prevent their use for complex disease analyses

[13]. Next, we evaluated the ability of LDSC to identify stratification in admixture mapping statistics through its intercept estimates and observed biased results with large variability (**Supplementary Figure 4**). We observed HAMSTA to have significantly greater power to detect stratification bias compared with LDSC (**Figure 2c**). For example, HAMSTA has 80% power when stratification explains 10% of PVE, compared with 5% power of LDSC. These relative differences in performance held when we increased the LAD score window size for LDSC **(Supplementary Figure 4)**. Overall, HAMSTA provides unbiased estimates of inflation in admixture mapping statistics due to ancestral bias and has greater power to reject its null compared to alternative approaches.

HAMSTA improves estimation of p-value thresholds to control family-wise error rate

As the number of approximately independent ancestry blocks depends on the demographic history of the population being studied, there is no universal threshold to determine genome-wide significance in admixture mapping studies. Admixture mapping often relies on permutation-based approaches to estimate the FWER, however these approaches can be computationally intractable for large datasets. Although a recently developed summary-static sampling scheme (STEAM) bypasses the need for individual-level permutations and speeds up the FWER estimation[20], its assumption that there exists no inflation in the test statistics may be unmet in the presence of population structure and polygenicity.

Here, we demonstrated inferences from HAMSTA can be leveraged to produce significance thresholds for association testing to achieve calibrated family-wise error rates (FWER) compared with STEAM. First, when PVE due to stratification is zero, we found STEAM and HAMSTA estimated similar significance thresholds (HAMSTA mean: 1.12×10^{-4}; STEAM: 1.57×10^{-4}), yielding comparable FWER at ~5% (**Figure 2d**), which suggests that HAMSTA-based FWER estimates do not deflate overall power despite increased model complexity. Importantly, in presence of ancestral stratification, we found HAMSTA estimates resulted in approximately calibrated FWERs unlike STEAM, which produced a considerable number of false positive associations (**Figure 2d, Supplementary Figure 6**). For example, when PVE due to stratification is 0.25, HAMSTA estimates resulted in FWER of 8% compared to the FWER of 34% from STEAM. Together, these findings demonstrate that intercepts estimated by HAMSTA can be incorporated into significance threshold estimation, producing better calibrated FWERs and therefore reducing false positive findings.

Application to African American in the PAGE study

To illustrate the ability of HAMSTA to estimate h_γ^2 from summary data, we applied it to admixture mapping summary statistics of 20 quantitative phenotypes computed from the African American participants in PAGE study[21] (mean N = 8383, SD N = 3901; see **Methods**). Briefly, we performed admixture mapping using 101,292 markers adjusting for the study center, global ancestry, and

phenotype-specific covariates. The average genomic inflation factor λ_{GC} across phenotypes is 1.53 (SD = 0.64). Next, we applied HAMSTA to generated summary statistics to infer h_γ^2 and evaluate potential stratification biases. To estimate h^2 from h_γ^2, we estimated the average African ancestry to be 78% and F_{STC} = 0.12 from the admixed individuals in PAGE and reference individuals from HGDP and 1000 Genomes.

We estimated the h_γ^2 ranges from 0.0025 for systolic blood pressure to 0.033 for height (mean h_γ^2 = 0.012; SE = 9.2×10^{-4}) across the 20 phenotypes, of which 13/20 were individually significantly different from 0 (nominal p-value < 0.05 in **Supplementary Table 1**). Translating h_γ^2 to estimates of h^2, we observed the h^2 ranging from 0.062 for systolic blood pressure to 0.85 for height (mean $h^2 = 0.30$; SE = 0.023), of which 13/20 were individually significant. We found these results were robust to different values of F_{STC} (see **Supplementary Table 1).**

Consistent with the simulation results, HAMSTA estimates were correlated more strongly with BOLT-REML estimates (r = 0.99, **Figure 3**) than those computed from LDSC (r = 0.44) (**Supplementary Figure 7**) This was largely attributable to statistical precision, with standard errors in HAMSTA estimates (range from 0.0023 to 0.014, mean = 0.0058) being slightly greater those from BOLT-REML (range from 0.0021 to 0.0076, mean = 0.0042), and noticeably lower than those computed from LDSC (range from 0.0064 to 0.021, mean = 0.012). Since 5/20 phenotypes had limited sample sizes (N<5,000), which is known to impact the performance of BOLT[26], we also estimated h_γ^2 using GCTA. Of the 16 estimates computed by GCTA that converged, we observed they were in general bounded by the estimates by HAMSTA and BOLT-REML (**Supplementary Figure 8**). Overall, we find that HAMSTA estimates of h_γ^2 are consistent with those computed from individual-level approaches in real data, while requiring much less computation time for the inference step (49 seconds for HAMSTA versus 51 minutes for GCTA).

To substantiate the translated h^2 estimates computed from HAMSTA, we compared with previous h^2 estimates reported from admixed individuals [11] as well as those from twin studies. Overall, we found our h^2 estimates are significantly correlated with the previously reported h_γ^2-based estimates [11] (r = 0.84, p=0.03). Focusing on height, and BMI, HAMSTA estimated h_γ^2 = 0.033 (se: 3.4×10^{-4}) and h_γ^2 = 0.017 (3.4×10^{-4}) respectively, corresponding to h^2 of 0.85 (0.085) and 0.42 (0.086) respectively. The estimated height h^2 was similar to the h^2 = 0.68 - 0.84 in twin studies [31], whereas the estimated BMI h^2 was smaller than the h^2 = 0.57 - 0.77 in twin studies [32] and higher than the h^2 = 0.30 in an estimation from whole-genome sequence data in European ancestry populations[33].

HAMSTA estimated intercepts suggested limited evidence for inflated summary statistics due to ancestral stratification in the admixture mapping (range from 0.97 to 1.01, average = 0.99; **Supplementary Table 1**), with 0/20 phenotypes differing significantly from the expectation of 1. Although LDSC suggested no significant deviation of intercepts from 1 (range from 0.18 to 1.95,

368 average = 1.07), individual intercepts varied more greatly under LDSC (mean SE = 0.34), than
369 those computed under HAMSTA (mean SE = 5.6×10^{-3}) (**Supplementary Table 1**).

370 Since in simulation we demonstrated that the significance threshold for admixture mapping
371 corresponding to FWER of 5% is sensitive to ancestral stratification, we estimated the thresholds
372 based on the HAMSTA intercepts. Under no ancestral stratification (i.e. intercept = 1), HAMSTA
373 estimated the significance threshold required to be 2.80×10^{-5}, which agrees with the threshold
374 of 2.10×10^{-5} reported by STEAM for African American[20]. Based on the estimated intercepts in
375 HAMSTA for the 20 phenotypes, the estimated thresholds range from 2.70×10^{-5} to 3.52×10^{-5}.
376 To conclude, HAMSTA found no evidence of inflation in admixture mapping statistics and
377 provided estimates for h_{γ}^{2} and hence h^{2} of the complex traits of African American in PAGE study.

378

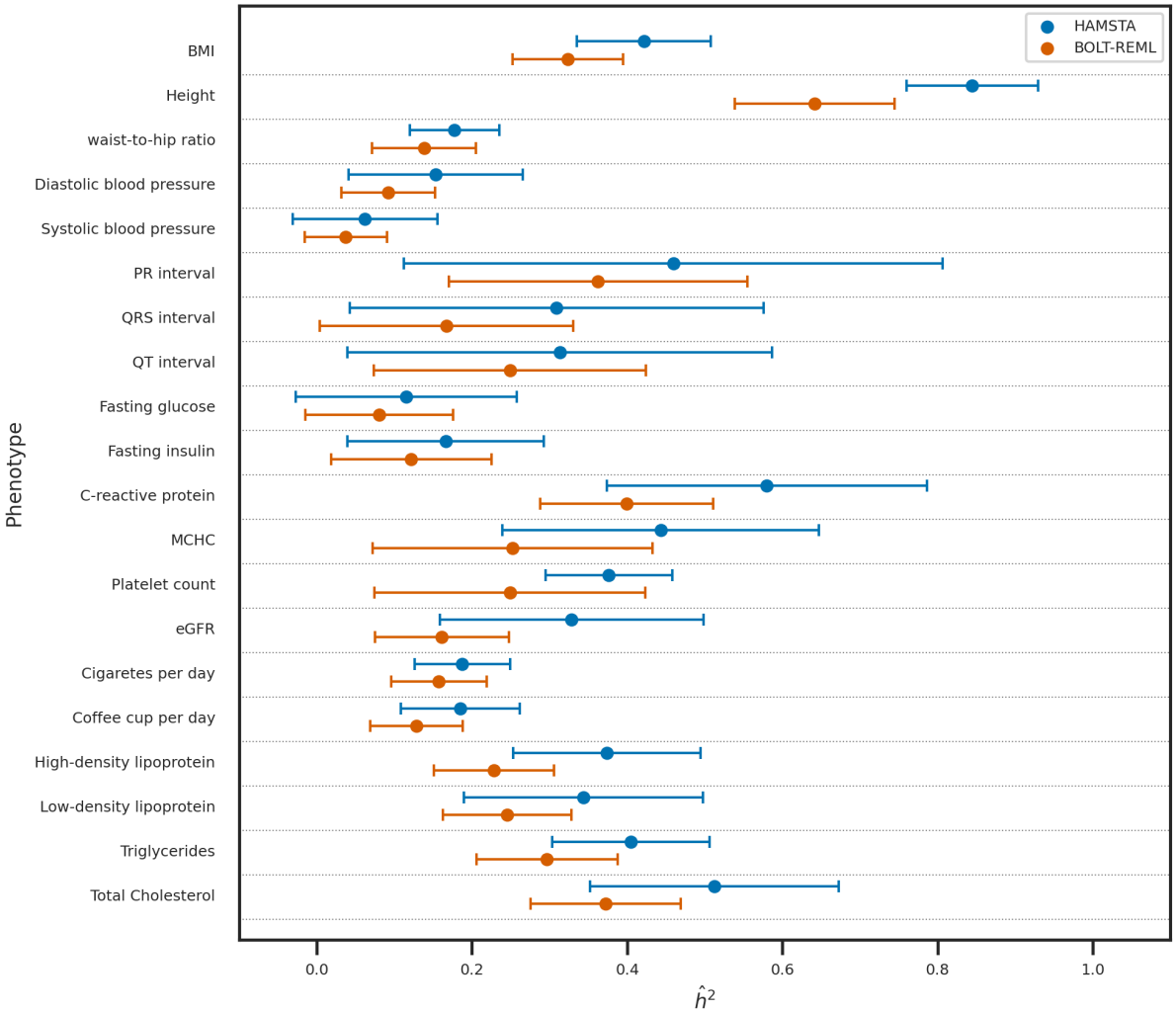

Figure 3

Comparison of $\hat{h}^2_\gamma$ -based $\hat{h}^2$between HAMSTA and BOLT-REML for the 20 quantitative traits in African American in PAGE. Results on 20 PAGE quantitative traits. Comparison between the estimates from HAMSTA, and BOLT-REML. Each point shows the $\hat{h}^2$, and the lengths of the error bars represent the standard errors.

Discussion

In this study, we demonstrated the use of summary statistics from admixture mapping to quantify the contribution of genetic variations to a trait. We developed a tool, HAMSTA, that unbiasedly estimate h^2_γ under the various trait architecture, including in the presence of unknown population

stratification in ancestral populations. Using the summary statistic-based approach, HAMSTA distinguishes the effect tagged by local ancestry on test statistics from unknown confounding biases. We also demonstrated that the estimated biases could be used to correct the significance threshold such that FWER are better controlled. Lastly, we applied HAMSTA to real-world data, showing that it can recover the h_γ^2 and hence h^2 from admixture mapping summary statistics.

Our method addresses several limitations in existing approaches estimating h_γ^2. First, because of the long-range correlations between local ancestry markers, LDSC requires a large window size to capture correlations with distant effect markers. Also, regression weights may not be sufficient to solve the problem of correlated χ^2 statistics, which could lead to inefficient estimation [34]. Our analysis shows that the efficiency can be improved when admixture mapping test statistics are rotated to an independent space. Second, REML could provide an unbiased estimate, but we showed in simulation that it is susceptible to ancestral stratification. Also, it is computationally expensive as the sample size increases. In real data analysis, the REML approach in GCTA failed to converge in waist-to-hip ratio, QT-interval, cigarette-per-day, and HDL. In contrast, we showed that HAMSTA would be a more robust approach to ancestral stratification and has no convergence problem in our analysis. Finally, existing methods assume uniform test statistics inflation although it has been shown that this assumption could be inaccurate [35,36]. HAMSTA relaxes this assumption by allowing multiple intercepts to represent non-uniform inflation. Overall, HAMSTA offers advantages over existing methods in the above aspects.

We are aware of several limitations of HAMSTA. First, HAMSTA only provides estimates of heritability explained by local ancestries in two-way admixtures, which may limit the use of the method in admixed populations with more than two ancestral populations. Currently, the relationship between h_γ^2 and h^2 are only established in two-way admixed populations such as African American, but models for h_γ^2 multi-way admixture has not yet been proposed. Incorporating the contribution of multiple ancestries in h_γ^2 and h^2 will be a possible extension in the future. Second, the standard error of HAMSTA h_γ^2 is larger than that from methods that use individual-level data like BOLT-REML (mean SE=0.0058 in HAMSTA versus mean SE=0.0042 in BOLT-REML). Nevertheless, HAMSTA h_γ^2 is robust to ancestral stratification, unlike BOLT-REML showing upward biases in the h_γ^2 estimates (**Figure 1d**). Third, HAMSTA only models summary statistics computed from linear regression on quantitative traits. The scope of this study is not extended to modeling binary traits. Future work can explore phenotypes under the liability-scale model and evaluate the use of summary statistics from logistic regression models. Lastly, since HAMSTA relies on an accurate LAD, factors that the LAD depends on, such as global ancestries, could potentially impact the accuracy of the estimates. These factors are required to be adjusted for when estimating the LAD.

In summary, our work opens a direction of summary statistics analysis in admixture mapping studies. Our method will facilitate studies of genetic architecture in large cohorts of admixed populations.

Acknowledgements

This work was funded in part by National Institutes of Health (NIH) under awards R01HG012133 and R35GM142783.

Web Resources

BOLT-REML, https://alkesgroup.broadinstitute.org/BOLT-LMM/BOLT-LMM_manual.html
GCTA, https://cnsgenomics.com/software/gcta/
GNOMAD HGDP and 1KG subsets, https://gnomad.broadinstitute.org/downloads#v3-hgdp-1kg
LDSC, https://github.com/bulik/ldsc
MSPRIME, https://github.com/tskit-dev/msprime
PLINK, https://www.cog-genomics.org/plink/
RFMIX2, https://github.com/slowkoni/rfmix
STEAM, https://github.com/kegrinde/STEAM

Data and code availability

The codes for HAMSTA are available at https://github.com/tszfungc/HAMSTA

References

1. Ziyatdinov, A., Parker, M.M., Vaysse, A., Beaty, T.H., Kraft, P., Cho, M.H., and Aschard, H. (2020). Mixed-model admixture mapping identifies smoking-dependent loci of lung function in African Americans. Eur. J. Hum. Genet. *28*, 656–668.

2. Nalls, M.A., Wilson, J.G., Patterson, N.J., Tandon, A., Zmuda, J.M., Huntsman, S., Garcia, M., Hu, D., Li, R., Beamer, B.A., et al. (2008). Admixture mapping of white cell count: genetic locus responsible for lower white blood cell count in the Health ABC and Jackson Heart studies. Am. J. Hum. Genet. *82*, 81–87.

3. Freedman, M.L., Haiman, C.A., Patterson, N., McDonald, G.J., Tandon, A., Waliszewska, A., Penney, K., Steen, R.G., Ardlie, K., John, E.M., et al. (2006). Admixture mapping identifies 8q24 as a prostate cancer risk locus in African-American men. Proc. Natl. Acad. Sci. U. S. A. *103*, 14068–14073.

4. Sofer, T., Baier, L.J., Browning, S.R., Thornton, T.A., Talavera, G.A., Wassertheil-Smoller, S., Daviglus, M.L., Hanson, R., Kobes, S., Cooper, R.S., et al. (2017). Admixture mapping in the Hispanic Community Health Study/Study of Latinos reveals regions of genetic associations with

461 blood pressure traits. PLoS One *12*, e0188400.

462 5. Galanter, J.M., Gignoux, C.R., Torgerson, D.G., Roth, L.A., Eng, C., Oh, S.S., Nguyen, E.A.,
463 Drake, K.A., Huntsman, S., Hu, D., et al. (2014). Genome-wide association study and admixture
464 mapping identify different asthma-associated loci in Latinos: The Genes-environments &
465 Admixture in Latino Americans study. Journal of Allergy and Clinical Immunology *134*, 295–305.

466 6. Pino-Yanes, M., Gignoux, C.R., Galanter, J.M., Levin, A.M., Campbell, C.D., Eng, C.,
467 Huntsman, S., Nishimura, K.K., Gourraud, P.-A., Mohajeri, K., et al. (2015). Genome-wide
468 association study and admixture mapping reveal new loci associated with total IgE levels in
469 Latinos. J. Allergy Clin. Immunol. *135*, 1502–1510.

470 7. Sun, H., Lin, M., Russell, E.M., Minster, R.L., Chan, T.F., Dinh, B.L., Naseri, T., Reupena,
471 M.S., Lum-Jones, A., Samoan Obesity, Lifestyle, and Genetic Adaptations (OLaGA) Study
472 Group, et al. (2021). The impact of global and local Polynesian genetic ancestry on complex
473 traits in Native Hawaiians. PLoS Genet. *17*, e1009273.

474 8. Shriner, D. (2017). Overview of Admixture Mapping. Curr. Protoc. Hum. Genet. *94*, 1.23.1-
475 1.23.8.

476 9. Shriner, D., Adeyemo, A., and Rotimi, C.N. (2011). Joint ancestry and association testing in
477 admixed individuals. PLoS Comput. Biol. *7*, e1002325.

478 10. Horimoto, A.R.V.R., Xue, D., Thornton, T.A., and Blue, E.E. (2021). Admixture mapping
479 reveals the association between Native American ancestry at 3q13.11 and reduced risk of
480 Alzheimer's disease in Caribbean Hispanics. Alzheimers. Res. Ther. *13*, 122.

481 11. Zaitlen, N., Pasaniuc, B., Sankararaman, S., Bhatia, G., Zhang, J., Gusev, A., Young, T.,
482 Tandon, A., Pollack, S., Vilhjálmsson, B.J., et al. (2014). Leveraging population admixture to
483 characterize the heritability of complex traits. Nat. Genet. *46*, 1356–1362.

484 12. Luo, Y., Li, X., Wang, X., Gazal, S., Mercader, J.M., 23 and Me Research Team, SIGMA
485 Type 2 Diabetes Consortium, Neale, B.M., Florez, J.C., Auton, A., et al. (2021). Estimating
486 heritability and its enrichment in tissue-specific gene sets in admixed populations. Hum. Mol.
487 Genet. *30*, 1521–1534.

488 13. Bulik-Sullivan, B.K., Loh, P.-R., Finucane, H.K., Ripke, S., Yang, J., Schizophrenia Working
489 Group of the Psychiatric Genomics Consortium, Patterson, N., Daly, M.J., Price, A.L., and
490 Neale, B.M. (2015). LD Score regression distinguishes confounding from polygenicity in
491 genome-wide association studies. Nat. Genet. *47*, 291–295.

492 14. Haak, W., Lazaridis, I., Patterson, N., Rohland, N., Mallick, S., Llamas, B., Brandt, G.,
493 Nordenfelt, S., Harney, E., Stewardson, K., et al. (2015). Massive migration from the steppe was
494 a source for Indo-European languages in Europe. Nature *522*, 207–211.

495 15. Browning, S.R., Grinde, K., Plantinga, A., Gogarten, S.M., Stilp, A.M., Kaplan, R.C., Avilés-
496 Santa, M.L., Browning, B.L., and Laurie, C.C. (2016). Local Ancestry Inference in a Large US-
497 Based Hispanic/Latino Study: Hispanic Community Health Study/Study of Latinos (HCHS/SOL).

498 G3 *6*, 1525–1534.

499 16. Berg, J.J., Harpak, A., Sinnott-Armstrong, N., Joergensen, A.M., Mostafavi, H., Field, Y.,
500 Boyle, E.A., Zhang, X., Racimo, F., Pritchard, J.K., et al. (2019). Reduced signal for polygenic
501 adaptation of height in UK Biobank. Elife *8*,.

502 17. Sohail, M., Maier, R.M., Ganna, A., Bloemendal, A., Martin, A.R., Turchin, M.C., Chiang,
503 C.W., Hirschhorn, J., Daly, M.J., Patterson, N., et al. (2019). Polygenic adaptation on height is
504 overestimated due to uncorrected stratification in genome-wide association studies. Elife *8*,.

505 18. Gopalan, S., Smith, S.P., Korunes, K., Hamid, I., Ramachandran, S., and Goldberg, A.
506 (2022). Human genetic admixture through the lens of population genomics. Philos. Trans. R.
507 Soc. Lond. B Biol. Sci. *377*, 20200410.

508 19. Speed, D., and Balding, D.J. (2019). SumHer better estimates the SNP heritability of
509 complex traits from summary statistics. Nat. Genet. *51*, 277–284.

510 20. Grinde, K.E., Brown, L.A., Reiner, A.P., Thornton, T.A., and Browning, S.R. (2019).
511 Genome-wide Significance Thresholds for Admixture Mapping Studies. Am. J. Hum. Genet.
512 *104*, 454–465.

513 21. Wojcik, G.L., Graff, M., Nishimura, K.K., Tao, R., Haessler, J., Gignoux, C.R., Highland,
514 H.M., Patel, Y.M., Sorokin, E.P., Avery, C.L., et al. (2019). Genetic analyses of diverse
515 populations improves discovery for complex traits. Nature *570*, 514–518.

516 22. Karczewski, K.J., Francioli, L.C., Tiao, G., Cummings, B.B., Alföldi, J., Wang, Q., Collins,
517 R.L., Laricchia, K.M., Ganna, A., Birnbaum, D.P., et al. (2020). The mutational constraint
518 spectrum quantified from variation in 141,456 humans. Nature *581*, 434–443.

519 23. Gravel, S., Henn, B.M., Gutenkunst, R.N., Indap, A.R., Marth, G.T., Clark, A.G., Yu, F.,
520 Gibbs, R.A., 1000 Genomes Project, and Bustamante, C.D. (2011). Demographic history and
521 rare allele sharing among human populations. Proc. Natl. Acad. Sci. U. S. A. *108*, 11983–
522 11988.

523 24. Kelleher, J., Etheridge, A.M., and McVean, G. (2016). Efficient Coalescent Simulation and
524 Genealogical Analysis for Large Sample Sizes. PLoS Comput. Biol. *12*, e1004842.

525 25. Chang, C.C., Chow, C.C., Tellier, L.C., Vattikuti, S., Purcell, S.M., and Lee, J.J. (2015).
526 Second-generation PLINK: rising to the challenge of larger and richer datasets. GigaScience *4*,.

527 26. Loh, P.-R., Bhatia, G., Gusev, A., Finucane, H.K., Bulik-Sullivan, B.K., Pollack, S.J.,
528 Schizophrenia Working Group of Psychiatric Genomics Consortium, de Candia, T.R., Lee, S.H.,
529 Wray, N.R., et al. (2015). Contrasting genetic architectures of schizophrenia and other complex
530 diseases using fast variance-components analysis. Nat. Genet. *47*, 1385–1392.

531 27. Yang, J., Lee, S.H., Goddard, M.E., and Visscher, P.M. (2011). GCTA: a tool for genome-
532 wide complex trait analysis. Am. J. Hum. Genet. *88*, 76–82.

533 28. Loh, P.-R., Danecek, P., Palamara, P.F., Fuchsberger, C., A Reshef, Y., K Finucane, H.,
534 Schoenherr, S., Forer, L., McCarthy, S., Abecasis, G.R., et al. (2016). Reference-based phasing
535 using the Haplotype Reference Consortium panel. Nat. Genet. *48*, 1443–1448.

536 29. Maples, B.K., Gravel, S., Kenny, E.E., and Bustamante, C.D. (2013). RFMix: a
537 discriminative modeling approach for rapid and robust local-ancestry inference. Am. J. Hum.
538 Genet. *93*, 278–288.

539 30. Shriner, D., Bentley, A.R., Doumatey, A.P., Chen, G., Zhou, J., Adeyemo, A., and Rotimi,
540 C.N. (2015). Phenotypic variance explained by local ancestry in admixed African Americans.
541 Front. Genet. *6*, 324.

542 31. Silventoinen, K., Sammalisto, S., Perola, M., Boomsma, D.I., Cornes, B.K., Davis, C.,
543 Dunkel, L., De Lange, M., Harris, J.R., Hjelmborg, J.V.B., et al. (2003). Heritability of adult body
544 height: a comparative study of twin cohorts in eight countries. Twin Res. *6*, 399–408.

545 32. Silventoinen, K., Jelenkovic, A., Sund, R., Yokoyama, Y., Hur, Y.-M., Cozen, W., Hwang,
546 A.E., Mack, T.M., Honda, C., Inui, F., et al. (2017). Differences in genetic and environmental
547 variation in adult BMI by sex, age, time period, and region: an individual-based pooled analysis
548 of 40 twin cohorts. Am. J. Clin. Nutr. *106*, 457–466.

549 33. Wainschtein, P., Jain, D., Zheng, Z., TOPMed Anthropometry Working Group, NHLBI Trans-
550 Omics for Precision Medicine (TOPMed) Consortium, Cupples, L.A., Shadyab, A.H., McKnight,
551 B., Shoemaker, B.M., Mitchell, B.D., et al. (2022). Assessing the contribution of rare variants to
552 complex trait heritability from whole-genome sequence data. Nat. Genet. *54*, 263–273.

553 34. Song, S., Jiang, W., Zhang, Y., Hou, L., and Zhao, H. (2022). Leveraging LD eigenvalue
554 regression to improve the estimation of SNP heritability and confounding inflation. Am. J. Hum.
555 Genet. *109*, 802–811.

556 35. Speed, D., Kaphle, A., and Balding, D.J. (2022). SNP-based heritability and selection
557 analyses: Improved models and new results. Bioessays *44*, e2100170.

558 36. Mathieson, I., and McVean, G. (2012). Differential confounding of rare and common variants
559 in spatially structured populations. Nat. Genet. *44*, 243–246.

560